journal

IR and XPS Studies on the Surface Structure of Poled ZnO–TeO$_2$ Glasses with Second-Order Nonlinearity

Aiko Narazaki

National Institute of Materials and Chemical Research, 1-1 Higashi, Tsukuba, Ibaraki 305-8565, Japan

Katsuhisa Tanaka

Department of Chemistry and Materials Technology, Faculty of Engineering and Design,
Kyoto Institute of Technology, Matsugasaki, Sakyo-ku, Kyoto 606-8585, Japan

Kazuyuki Hirao*

Department of Material Chemistry, Graduate School of Engineering, Kyoto University,
Sakyo-ku, Kyoto 606-8501, Japan

Tadanori Hashimoto, Hiroyuki Nasu, and Kanichi Kamiya

Department of Chemistry for Materials, Faculty of Engineering, Mie University, Kamihama, Tsu, Mie 514-8507, Japan

The effect of thermal/electrical poling on the surface structure of 30ZnO·70TeO$_2$ glass has been investigated by means of IR reflectance and X-ray photoelectron spectroscopy (XPS). All the poled glasses exhibit a common characteristic that the second-order nonlinearity is induced preferentially in an anode-side surface region. The reflectance from the anode-side glass surface at around 635 cm^{-1} assignable to the vibrational mode of the Te–O$_{ax}$ bond, where ax stands for the axial position of the TeO$_4$ trigonal bipyramid, is smaller in comparison with both as-annealed and cathode-side surfaces. The XPS analysis on the anode-side surface shows a depletion of Zn^{2+} ions and penetration of Na$^+$ ions from the borosilicate glass which was placed between the sample and the anode during poling. These results suggest that the poling brings about both the breaking of the tellurite glass network and compositional changes at the anode-side surface below which the second-order nonlinearity is preferentially induced.

I. Introduction

THERMAL/ELECTRICAL poling is one of the attractive tools for fabrication of glass materials with useful electrooptical properties as well as optical second-order nonlinearities.[1–4] Poled tellurite glasses[5–10] as well as silica-based glasses exhibit second-harmonic generation (SHG) and possibly allow one to achieve large second-order nonlinearity because of large third-order nonlinear susceptibility, $\chi^{(3)}$, which contributes to second-order nonlinearity when SHG can be induced predominantly by a process of $\chi^{(2)}_{\text{eff}} = 3\chi^{(3)} \cdot E_{\text{dc}}$. A peculiar dependence of second-harmonic intensity on poling temperature is observed in all of the tellurite glasses that we examined thus far;[8–10] when the poling temperature increases, the second-harmonic intensity increases, manifests a maximum, and decreases just below its glass transition temperature. Moreover, there is a linear relation between the glass transition temperature and the optimum poling temperature where the second-harmonic intensity becomes a maximum.

In addition to the practical interest, many researchers have been attracted to the SHG-active structure developed in glass which is originally a prototype of SHG-inactive material. Nowadays, the following aspect of the induction mechanism of SHG is generally accepted for oxide glasses. The SHG-active region can be formed preferentially beneath an anode-side glass surface. However, the problem of how and which ions in the vicinity of the anode-side surface are affected by a high dc electric field during poling is left open. A clarification of this problem makes the SHG-active structure clearer.

The present work was performed to examine the surface structure of poled 30ZnO·70TeO$_2$ glass with second-order nonlinearity. As revealed in our previous paper,[10] when an anode-side surface of the 30ZnO·70TeO$_2$ glass poled at 280°C for 20 min was etched mechanically to a thickness of about 30 μm, the second-order nonlinearity disappeared. In addition, variation of the second-harmonic intensity with the angle of incidence could be fitted using the Maker fringe theory on the assumption that second-order nonlinearity was effectively induced within a thin layer 27 μm thick. From these facts, it can be deduced that the modification of the tellurite glass structure was caused by the thermal/electrical poling preferentially at the surface region, as mentioned above for the general oxide glasses. We chose this composition because the decay of second-harmonic intensity was barely observed for this glass even about 1 year after poling.[10] An infrared (IR) reflectance technique was used to explore the glass network structure at the near-surface region of the poled 30ZnO·70TeO$_2$ glass. TeO$_4$ trigonal bipyramids are the basic structural unit of tellurite glasses and they are connected with each other in three-dimensional space, leading to the glass network structure. On the other hand, an addition of network-modifying oxides such as ZnO gives rise to TeO$_3$ trigonal pyramids which are considered to restrict glass formation. Thus, we can see IR reflectance peaks attributable to two types of TeO$_n$ polyhedra.[11] Hence, by using IR technique, we may detect a change in glass network structure caused by poling. Also, X-ray photoelectron spectroscopy (XPS) was conducted for the purpose of probing the concentration of each glass-constituent atom for the as-annealed and poled glasses.

R. K. Brow—contributing editor

II. Experimental Procedure

Glass samples were prepared from ZnO and TeO$_2$ as starting materials by using the conventional melt-quenching method. The purity was 99% and 99.9%, respectively. The powders of raw materials were mixed thoroughly to make a nominal composition of 30ZnO·70TeO$_2$ and melted in a platinum crucible at 900°C for 20 min in air. The melt was rapidly cooled by pouring onto a carbon plate to obtain glass. The glass was annealed for 20 min at 345°C, which is around its glass transition temperature, T_g = 326°C, determined using differential thermal analysis (Rigaku, TG-DTA8112BH). The cooling rate from annealing temperature was about 3 K/min. The as-annealed glass was cut into a plate, and then both surfaces of the platelike glass were polished with aqueous suspension of CeO$_2$ for optical measurements. The resultant glass specimen had a thickness of 1 mm.

Poling of the glass sample was performed as follows. The glass sample was sandwiched in between two commercial borosilicate glass plates with a thickness of 0.15 mm and contacted physically with electrodes made of stainless steel. The commercial borosilicate glass plates were used to avoid precipitation of metallic tellurium, which occurred on the cathode-side glass surface when the glass sample was directly brought into contact with the electrodes made of stainless steel. The use of commercial borosilicate glass plates was also effective to avoid discharge between the electrodes. The glass sample sandwiched with the electrodes was put into an electric furnace and heated at an aimed temperature for 30 min. The poling temperature was in the range of 260°–300°C, which is 26°–66°C lower than the glass transition temperature. After a voltage of 3 kV was applied for 40 min at the temperature, the glass sample was taken out from the furnace and kept at room temperature for 60 min with the voltage applied. It should be noted that the actual voltage applied to the sample was estimated to be 1.7 kV, when the dielectric constants of 30ZnO·70TeO$_2$ and borosilicate glasses were assumed to be 21[12] and 7.9,[13] respectively.

Both the as-annealed and poled glass specimens thus obtained were subjected to IR and XPS measurements. The IR reflectance spectra were measured with an FT-IR spectrometer (Japan Spectroscopic, FT/IR-550) in the wavenumber range of 4000 to 400 cm^{-1} in air. Samples were placed so that the angle of incidence was 10°. The reference was an aluminum mirror. The obtained data were corrected by subtracting the reflectance due to atmospheric CO$_2$. The glass composition was investigated with an XPS (ULVAC-phi, MT-5500) using MgKα X-ray as an excitation source under a pressure of 10^{-9} torr.

Second-harmonic generation of the poled glass samples was measured using the Maker fringe method. A pulsed Nd:YAG laser (Spectra Physics, GCR-11), which operated in a Q-switched mode with a 10 Hz repetition rate, was used as a light source. After a pulse at 1064 nm with 9 ns duration was p-polarized, it was incident on the sample at −65° to 65°. The beam diameter was about 1 mm. The output light from the poled glass sample was passed through both an IR cut filter and a monochromator (Spex, 270M) to eliminate the fundamental wave at 1064 nm completely. The second-harmonic wave at 532 nm was detected with a photomultiplier (Hamamatsu Photonics, R955). The signal from the photomultiplier was integrated by using a digital oscilloscope (Hewlett-Packard, 54522A). The second-harmonic intensity from Y-cut quartz with a thickness of 1.046 mm and d_{11} = 0.34 pm/V was also measured for the purpose of determining input light power.

III. Results

Figure 1 shows the reflectance spectra in the range of 4000–400 cm^{-1} for as-annealed and poled 30ZnO·70TeO$_2$ glasses. In the spectral range of 3500–1800 cm^{-1}, the Kramers–Kronig conversion was conducted to calculate the imaginary part of the complex refractive index, $n - ik$, under the requirement that there is no significant change of reflectance at both ends of the spectral
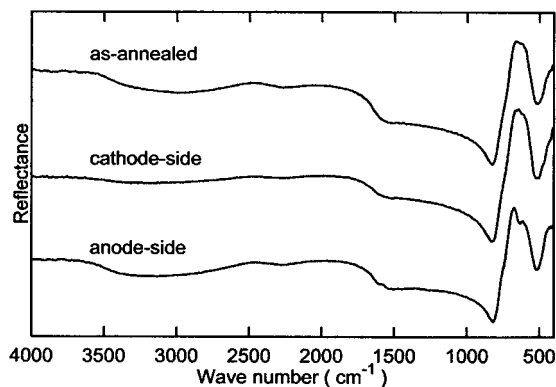

Fig. 1. Reflectance spectra from 4000 to 400 cm^{-1} for 30ZnO·70TeO$_2$ glasses. The spectra from the top to the bottom correspond to the reflectance from as-annealed, cathode-side, and anode-side surfaces, respectively. The poling was conducted at 280°C for 40 min.

region.[14] The wavenumber dependence of k thus obtained is shown in Fig. 2. Bürger *et al.* reported that the absorption band caused by free OH groups appeared in the vicinity of 3000 cm^{-1} for several tellurite glasses.[15] In this work, a peak of k was observed at around 2700 cm^{-1} for all of the glasses used and assigned to the vibration of free OH groups. Moreover, the peak intensity decreased slightly at the cathode-side surface after poling, whereas the intensity for the anode side was comparable with that of the as-annealed surface. This suggests that the poling brought about a decrease in the OH amount at the cathode side. However, it should be mentioned that further measurements without the influence of atmospheric H$_2$O is needed to discuss in detail the poling effect on the amount of water inside the glass.

The reflectance spectra from 1400 to 400 cm^{-1} are shown in Fig. 3. A broad reflectance peak at 700–600 cm^{-1} was observed in all of the spectra. The reflectance around 600 cm^{-1} from the anode-side surface is smaller compared with both the as-annealed and cathode-side surfaces. Mochida *et al.* reported transmission IR spectra from 4000 to 350 cm^{-1} for 30ZnO·70TeO$_2$ glass;[11] the absorption at 635 and 675 cm^{-1} can be assigned to the vibrational modes of the Te–O$_{ax}$ bond in TeO$_4$ trigonal bipyramid and the Te–O bond in TeO$_3$ trigonal pyramid, respectively. Thus, the above-described broad peak at 700–600 cm^{-1} can be identified as a superposition of both the reflectance at 635 and 675 cm^{-1} due to Te–O$_{ax}$ and TeO$_3$, respectively. Therefore, the decrease in reflectance at 635 cm^{-1} at the anode-side surface suggests a breaking of Te–O$_{ax}$ bonds after poling.

Figure 4 shows the IR reflectance for the anode-side surface etched to a thickness of 5 μm. The intensity at 635 cm^{-1} recovered after the mechanical etching. This indicates that the decrease in the relative number of Te–O$_{ax}$ bonds takes place just beneath the anode-side surface.
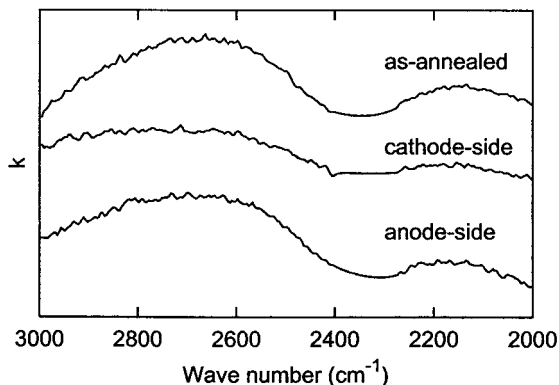

Fig. 2. Imaginary part, k, of the complex refractive index obtained by the Kramers–Kronig conversion of IR reflectance spectra for as-annealed and poled glasses.
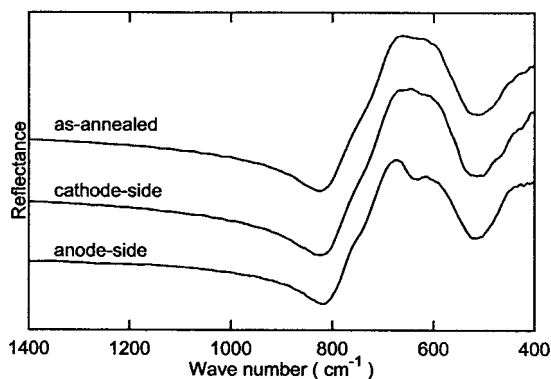
Fig. 3. Reflectance spectra from 1400 to 400 cm^{-1} for both as-annealed and poled 30ZnO·70TeO$_2$ glasses.
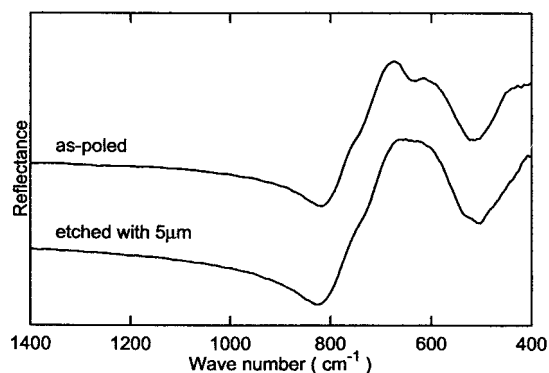

Fig. 4. IR reflectance from anode-side surface of the poled 30ZnO·70TeO$_2$ glass after the original surface was removed mechanically with a thickness of 5 μm.

Table I lists the concentration ratios of network-modifying cations estimated from the XPS data for both as-annealed and anode-side surfaces. The atomic concentration was obtained from the peak area divided by atomic sensitivity. To discuss the change in the number of Zn and Na ions, their concentrations were normalized by that of Te ions on the assumption that the number of Te ions is not varied throughout the bulk glass even after poling. The error in these ratios is ±0.005. The concentration ratio of Zn to Te for the as-annealed glass is lower than that estimated for 30ZnO·70TeO$_2$ glass composition. With this in mind, we will discuss the poling effect on the glass composition by comparing the concentration ratios of the poled glasses with that obtained from the XPS measurements for the as-annealed one. The concentration of Zn^{2+} ions in poled glasses is lower than that of the original glass. Although the original glass does not contain sodium ions except those as impurities, an increase in Na$^+$ content is observed at the anode side in comparison with the as-annealed

glass. It is feasible that this increase is due to the penetration of Na$^+$ from the borosilicate glass which was placed between the anode and tellurite glass sample during the poling.

The variation in the concentration ratio at cathode-side surface is shown in Table II. The concentration of Zn^{2+} ions increases compared with the as-annealed glass, whereas the ratio of Na$^+$ is lower than that of the anode side.

The dependence of second-harmonic intensity on incident angle, namely, the Maker fringe pattern, is depicted for poled 30ZnO·70TeO$_2$ glasses in Fig. 5. The solid curve and closed and open circles denote the Maker fringe patterns corresponding to the poling temperatures of 260°, 280°, and 300°C, respectively. The second-harmonic intensity manifests a maximum at a certain temperature which we define as the optimum poling temperature. This behavior is similar to those of various tellurite glasses reported previously.[8-10] In the present case, the optimum poling temperature is 280°C, which is about 50°C below the glass transition temperature.

IV. Discussion

Poling induces second-order nonlinearity in various kinds of tellurite glasses. The SHG-active region exists mainly in a thin layer beneath the anode-side surface in poled tellurite as well as in other poled oxide glasses. For instance, the SHG-active layer ranged from the anode-side surface to 27 μm depth in the 30ZnO·70TeO$_2$ glass poled at 280°C for 20 min.[10] As for silica glass, Liu *et al.* revealed that the thickness of a SHG-active layer increased from 5.8 up to 14 μm with increasing poling voltage when the poling temperature was set at 275°C.[16]

One possible explanation for the localization of the induced second-order nonlinearity is as follows. When an external voltage is applied during poling, relatively mobile cations in glasses such as Na$^+$ drift toward a cathode to screen the applied voltage. Assuming a blocking anode,[17,18] this results in the creation of a cation-depleted layer with net minus charge at the anode side because the anions in oxide glasses, i.e., nonbridging oxygens, are stuck more strongly to the glass network and immobile. The depleted region at the anode-side surface creates second-order nonlinear susceptibility, $\chi_{\text{eff}}^{(2)}$, via the process represented by the following equation:

$$\chi_{\text{eff}}^{(2)} = 3\chi^{(3)} \cdot E_{\text{dc}} \tag{1}$$

where $\chi^{(3)}$ is the third-order nonlinear susceptibility that the tellurite glasses originally possess, and E_{dc} is the frozen electric field in the cation-depleted region. It has also been proposed that second-order nonlinearity can be induced by the orientation of dipole moments in a glass network along an external field. Although it is still unclear which process is predominant to form a SHG-active layer in various kinds of oxide glasses, the former or the latter, the preferential formation of the SHG-active region just below the anode-side surface suggests that the glass surface can be drastically modified by poling and profoundly related to the induced second-order nonlinearity.

The IR reflectance from the anode-side surface depicted in Fig. 1 shows a decrease in intensity at around 635 cm^{-1} assigned to the

Table I. Concentration Ratio of Modifying Cations to Te for Anode-Side and As-Annealed Surfaces of 30ZnO·70TeO$_2$ Glasses

Poling temperature (°C)	Concentration ratio	
	Zn/Te	Na/Te
260	0.13	0.09
280	0.10	0.10
300	0.11	0.10
As-annealed	0.14	0.04

Table II. Concentration Ratio for Cathode-Side Surfaces of Poled 30ZnO·70TeO$_2$ Glasses

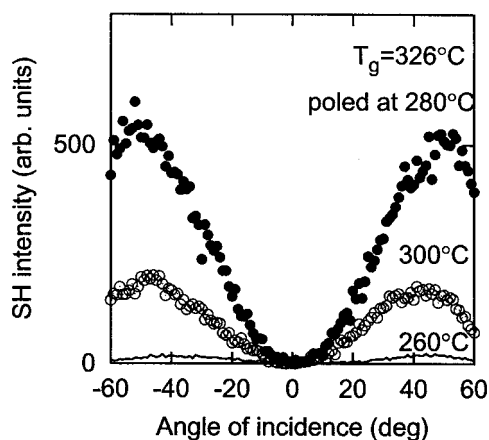| Poling temperature (°C)	Concentration ratio	
	Zn/Te	Na/Te
280	0.19	0.08
300	0.19	0.03
As-annealed	0.14	0.04

Fig. 5. Variation of second-harmonic intensity with incident angle, namely, Maker fringe pattern for poled 30ZnO·70TeO$_2$ glasses. The solid curve and closed and open circles represent the second-harmonic intensity for the specimens poled at 260°, 280°, and 300°C, respectively.

vibration mode of the Te–O$_{ax}$ bond in TeO$_4$ trigonal bipyramid in the ZnO–TeO$_2$ system.[11] According to this assignment, it can be concluded that poling treatment brought about a breaking of the tellurite glass network.

Mochida *et al.* also reported the dependence of IR absorption on ZnO and Na$_2$O content in ZnO–TeO$_2$ and Na$_2$O–TeO$_2$ binary glass systems; when ZnO or Na$_2$O content became higher, the absorption assigned to the Te–O$_{ax}$ bond decreased, accompanied by an increase in absorption at around 675 cm^{-1} assigned to the Te–O bonds in TeO$_3$ polyhedra. However, the poled 30ZnO·70TeO$_2$ glasses used in the present experiments did not show the increase in intensity at 675 cm^{-1}. Hence, the decrease in Te–O$_{ax}$ bonds was caused not only by a change in the amount of network-modifying cations but also by an additional poling effect. Moreover, the fact that the reflectance at 635 cm^{-1} recovered after the anode-side surface was removed with 5 μm thickness indicates that the structural change observed by IR spectroscopy is restricted in a thin layer below the anode-side surface.

The glass compositions obtained for the anode-side surface in Table I exhibit common characteristics irrespective of the poling temperature. The percentage of Zn decreased by about 30% after poling, whereas the ratio of Na in poled glass became twice as large as that of the as-annealed one. In contrast to the results for the anode-side surface, the evaluated compositions for the cathode side show that the concentration of Zn is higher than that of the as-annealed surface (Table II). Therefore, it can be speculated that when the external electric field is applied, Zn^{2+} cations drift toward the cathode to screen the external electric field followed by their depletion and accumulation at the anode- and cathode-side surfaces, respectively. As for Na$^+$ ions implanted from the borosilicate glass placed between the anode and the tellurite glass sample, they are conducted through the tellurite glass, making a slight accumulation in the vicinity of the anode-side surface. Consequently, the poling treatment creates Zn^{2+}-ion-depleted and Na$^+$-ion-accumulated regions at the anode-side surfaces. Although it is still difficult to discuss the net charge left at the anode-side surface after poling, the induced second-order nonlinearity can also be explained by a redistribution of the modifying cations which forms a frozen electric field and contributes to second-order nonlinearity via the process in Eq. (1).

As shown in Fig. 5, the second-harmonic intensity exhibits a maximum at the optimum poling temperature, 280°C. According to the XPS data of the anode side, the ratio of Zn is the least at the optimum poling temperature, possibly leading to a freeze of the largest static electric field and then the largest SHG among the present glasses.

V. Conclusions

The effect of poling on the surface structure was investigated by means of IR reflectance and X-ray photoelectron spectroscopy for 30ZnO·70TeO$_2$ glasses with second-order nonlinearity. Since second-order nonlinearity is apt to be induced in the vicinity of the anode-side glass surface, information on its surface structure is required to study the origin of the second-harmonic generation.

In the IR reflectance spectra, it was observed that the intensity at around 635 cm^{-1} decreased at the anode-side surface in comparison with the as-annealed and cathode-side surfaces. This means a decrease in the number of Te–O$_{ax}$ bonds. In other words, poling caused the breaking of the tellurite glass network at the anode-side surface. However, this change in reflectance disappeared after etching of the anode-side surface to a 5 μm thickness. Another influence of poling is the modification of glass composition. The XPS data of the anode-side revealed a depletion of Zn^{2+} ions and an increase in the number of Na$^+$ ions moved from the borosilicate glass, which was placed between the sample and the anode during poling.

From these results, it was revealed that poling significantly affects both the glass network and composition, resulting in the induction of second-order nonlinearity. Further measurements of the depth profile of the glass composition and SHG will be needed to discuss in detail how second-order nonlinearity can be induced.

References

[1]R. A. Myers, N. Mukherjee, and S. R. J. Brueck, "Large Second-Order Nonlinearity in Poled Fused Silica," *Opt. Lett.*, **16**, 1732–34 (1991).

[2]H. Nasu, H. Okamoto, A. Mito, J. Matsuoka, and K. Kamiya, "Influence of the OH Content on Second Harmonic Generation from Electrically Polarized SiO$_2$ Glasses," *Jpn. J. Appl. Phys.*, **32**, 180–81 (1993).

[3]H. Takebe, P. G. Kazansky, and P. S. J. Russell, "Effect of Poling Conditions on Second-Harmonic Generation in Fused Silica," *Opt. Lett.*, **21**, 468–70 (1996).

[4]A. Okada, K. Ishii, K. Mito, and K. Sasaki, "Phase-Matched Second-Harmonic Generation in Novel Corona Poled Glass Waveguides," *Appl. Phys. Lett.*, **60**, 2853–55 (1992).

[5]K. Tanaka, K. Kashima, K. Hirao, N. Soga, A. Mito, and H. Nasu, "Second-Harmonic Generation in Poled Tellurite Glasses," *Jpn. J. Appl. Phys.*, **32**, L843–45 (1993).

[6]K. Tanaka, A. Narazaki, K. Hirao, and N. Soga, "Poling Temperature Dependence of Optical Second-Harmonic Intensity of MgO–ZnO–TeO$_2$ Glasses," *J. Appl. Phys.*, **79**, 3798–800 (1996).

[7]K. Tanaka, A. Narazaki, K. Hirao, and N. Soga, "Optical Second Harmonic Generation in Poled MgO–ZnO–TeO$_2$ and B$_2$O$_3$–TeO$_2$ Glasses," *J. Non-Cryst. Solids*, **203**, 49–54 (1996).

[8]A. Narazaki, K. Tanaka, K. Hirao, and N. Soga, "Effect of Poling Temperature on Optical Second Harmonic Intensity of Sodium Zinc Tellurite Glasses," *J. Appl. Phys.*, **83**, 3986–90 (1998).

[9]A. Narazaki, K. Tanaka, K. Hirao, and N. Soga, "Effect of Poling Temperature on Optical Second-Harmonic Intensity of Lithium Sodium Tellurite Glass," *J. Am. Ceram. Soc.*, **81**, 2735–37 (1998).

[10]A. Narazaki, K. Tanaka, K. Hirao, and N. Soga, "Induction and Relaxation of Optical Second-Order Nonlinearity in Tellurite Glasses," *J. Appl. Phys.*, **85**, 2046–51 (1999).

[11]N. Mochida, K. Takahashi, K. Nakata, and S. Shibusawa, "Properties and Structure of the Binary Tellurite Glasses Containing Mono- and Divalent Cations," *J. Ceram. Soc. Jpn.*, **86**, 316–26 (1978).

[12]M. J. Redman and J. H. Chen, "Zinc Tellurite Glasses," *J. Am. Ceram. Soc.*, **50**, 523–25 (1967).

[13]A. A. Appen and G. Fuxi, "Electrical Properties in R$_2$O–R$_2$O$_3$–SiO$_2$ Systems"; pp. 516–17 in *Handbook of Glass Data, Part C, Ternary Silicate Glasses*. Elsevier Science Publishers B.V., Amsterdam, Netherlands, 1987.

[14]D. M. Roessler, "Kramers–Kronig Analysis of Reflectance Data III. Approximations, with Reference to Sodium Iodide," *Br. J. Appl. Phys.*, **17**, 1313–17 (1966).

[15]H. Bürger, W. Vogel, and V. Kozhukharov, "IR Transmission and Properties of Glasses in the TeO$_2$–[R$_n$O$_m$, R$_n$X$_m$, R$_n$(SO$_4$)$_m$, R$_n$(PO$_3$)$_m$ and B$_2$O$_3$] Systems," *Infrared Phys.*, **25**, 395–409 (1985).

[16]A. C. Liu, D. Pureur, M. J. F. Digonnet, G. S. Kino, and E. J. Knystautas, "Improving the Nonlinearity of Silica by Poling at Higher Temperature and Voltage"; pp. 302–304 in OSA Technical Digest Series, Vol. 17, *Bragg Gratings, Photosensitivity, and Poling in Glass Fibers and Waveguide: Applications and Fundamentals*. Optical Society of America, Washington, DC, 1997.

[17]D. E. Carlson, "Ion depletion of Glass at a Blocking Anode: I, Theory and Experimental Results for Alkali Silicate Glasses," *J. Am. Ceram. Soc.*, **57**, 291–94 (1974).

[18]D. E. Carlson, K. W. Hang, and G. F. Stockdale, "Ion Depletion of Glass at a Blocking Anode: II, Properties of Ion-Depleted Glasses," *J. Am. Ceram. Soc.*, **57**, 295–300 (1974). □